

## 2 Network Configurations and Models

**Abstract** The objective of this chapter is to review the basic configurations of power networks. In particular, transmission and distribution lines are considered. The first ones are usually built as overhead lines. Different configurations of such lines are described in detail: single- and double-circuit lines, multi-terminal and tapped lines, traditional and series-compensated transmission lines. Lumped- and distributed-parameter models of the lines are presented. Basic features related to distribution networks are presented.

### 2.1 Introduction

Specific features of lines used in contemporary power systems depend on many factors, such as their construction (overhead or cable, materials used and line geometry), voltage level (generally: high voltage or medium voltage), network configurations (single-circuit, double-circuit, two- or multi-terminal lines, tapped lines), reactance compensation (uncompensated or series-compensated) and others. All these details should be taken into considerations when the network mathematical models for steady-state and transients are formulated. These models, together with the respective measurement procedures, which are introduced in Chap. 4, constitute the basis for the fault-location algorithms. This chapter gives an overview of different types of lines and their models from the fault-location point of view.

### 2.2 Overhead Lines

Fault location in transmission networks is based on considering the flow of a fault current. Depending on the availability of measurements for the fault locator, the flow of a fault current within the faulted line itself or also in its vicinity is considered. A particular fault-location method has to be considered in strict relation to the configuration of the power network and its model.

### 2.2.1 Single-circuit Overhead Lines

Single-circuit three-phase overhead lines are the simplest means for transmitting power energy from the generation center to the consumption region. A schematic diagram of a power network with a single-circuit overhead line is presented in Fig. 2.1a [11]. The line is marked with a graphic symbol typical of an impedance description. Moreover, the description  $\underline{Z}_L$ , corresponding to a general indication of the line impedance is used. The line ends are denoted here by letters: A and B. The fault occurring on the line is marked with a common graphic symbol for the fault and letter F. The vicinity of the line A–B under consideration is represented by the external network. Assuming linearity of the whole circuit, the external network can be equivalented [11], as shown in Fig. 2.1b. The obtained equivalent of the external network in a general case consists of:

- two equivalent sources behind the line terminals A, B – consisting of the emfs ( $\underline{E}_A$ ,  $\underline{E}_B$ ) and source impedances ( $\underline{Z}_A$ ,  $\underline{Z}_B$ ); and
- extra link ( $\underline{Z}_E$ ) between the line terminals A, B.

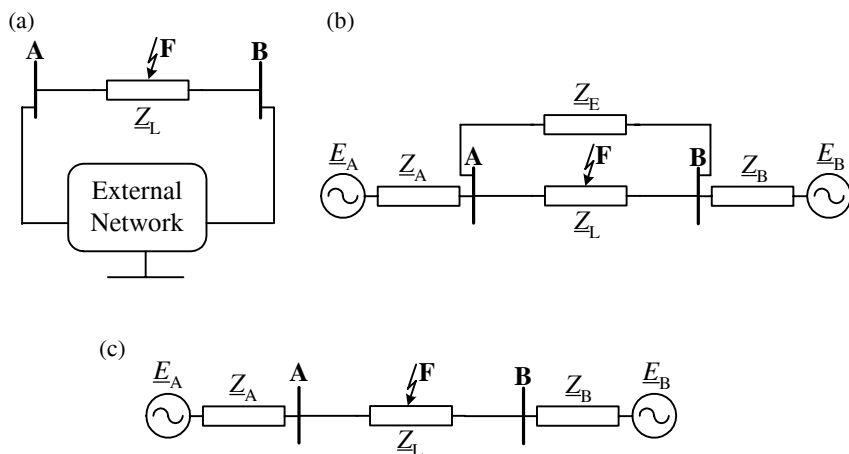


**Fig. 2.1** Transmission network with single-circuit overhead line: (a) generic scheme, (b) general equivalent scheme, and (c) simplified equivalent scheme with the line being the only connection between buses A, B

Since the load and generation in a power network as well as the network topology undergo changes, the equivalent network of the line external network also changes and is not fixed. As a result, the source impedances ( $\underline{Z}_A$ ,  $\underline{Z}_B$ ) are considered in the fault-location process to be the uncertain parameters. Therefore, the fault-location algorithms, which do not require that the source impedances be known, are generally more accurate than the algorithms for which this impedance data is used as the input data. The one-end fault-location algorithms require setting the source impedances and due to dynamic changes of the network it is difficult to provide the actual values of these impedances. Fortunately, in many applications it

is sufficient to provide the representative values of the source impedances, which are obtained for the most typical conditions of the network operation. Possible mismatch between the provided representative source impedances and the actual parameters in many applications does not cause considerable errors in fault location. This is so especially in the case of strong sources, which is the case when the source impedance is much smaller than the line impedance.

If the line ( $\underline{Z}_L$ ) considered is the only connection between the buses A, B, then the extra link ( $\underline{Z}_E$ ) does not exist, and there are only equivalent sources, as shown in Fig. 2.1c. This is the well-known double-machine network.

### 2.2.2 Double-circuit Lines

Both fault location and protective relaying for double-circuit lines (also called parallel lines) are dealt with in numerous references [7, 29, 68, 76, 90, 106, 109, 113, 114, 121, 122, 131, 140, 155, 204, 205, 218, 286, 293, 294, 299, 344]. Such lines are basically constructed due to constraints in obtaining new right-of-ways and are very common in power networks. For such lines the two three-phase transmission circuits are arranged on the same tower or follow on adjacent towers the same right-of-way. The circuits may be either of the same or different voltage level. Also, more than two three-phase circuits can be arranged in such a way (multi-circuit lines) [350].

Due to the nearness of both circuits of a double-circuit line, they are mutually magnetically coupled. The magnetic coupling is related to the effect of a current flowing in one circuit, which influences the voltage profile in the other circuit, and *vice versa*. This means that the voltage profile of a given circuit is not entirely dependent on the current flowing in this circuit.

The mutual coupling effect can be expressed in terms of various inter-circuit mutual impedances. Using the symmetrical components approach to the line description, the positive-, negative- and zero-sequence mutual impedances are considered. The positive- and negative-sequence mutual impedances are usually a small fraction of the positive-, negative-sequence self-impedances and therefore are usually neglected in the analysis. In contrast, the zero-sequence mutual impedance ( $\underline{Z}_{0m}$ ) is of relatively high value and thus cannot be ignored in the analysis of single phase-to-ground faults. The mutual coupling of double-circuit lines for the zero-sequence is thus important for the fault location based on considering the natural fault loops [109].

Different configurations of double-circuit lines [11, 109, 350] are met in power networks. Figure 2.2 presents a general configuration of a power network with a double-circuit overhead line terminated on both sides at the separate buses. The line circuits are denoted by  $\underline{Z}_{L,I}$ ,  $\underline{Z}_{L,II}$  and their mutual coupling for the zero-sequence by  $\underline{Z}_{0m}$ . The vicinity of the line circuits is represented with:

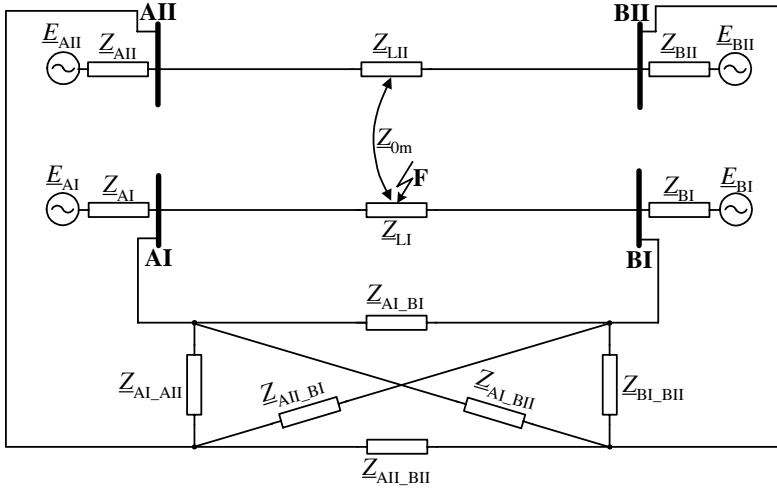


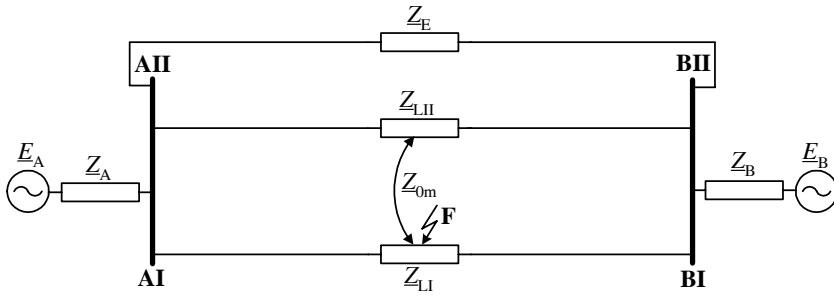
**Fig. 2.2** Schematic diagram of power network with double-circuit overhead line terminated at both ends at separate buses

- equivalent source behind the line terminal AI (emf:  $\underline{E}_{AI}$ , impedance:  $\underline{Z}_{AI}$ );
- equivalent source behind the line terminal AII (emf:  $\underline{E}_{AII}$ , impedance:  $\underline{Z}_{AII}$ );
- equivalent source behind the line terminal BI (emf:  $\underline{E}_{BI}$ , impedance:  $\underline{Z}_{BI}$ );
- equivalent source behind the line terminal BII (emf:  $\underline{E}_{BII}$ , impedance:  $\underline{Z}_{BII}$ ); and
- links between the line terminals AI, AII, BI, BII in the form of a complete tetragonal of impedances:  $\underline{Z}_{AI\_AII}$ ,  $\underline{Z}_{AI\_BI}$ ,  $\underline{Z}_{AI\_BII}$ ,  $\underline{Z}_{AII\_BI}$ ,  $\underline{Z}_{AII\_BII}$ ,  $\underline{Z}_{BI\_BII}$ .

Figure 2.3 presents the classical case of the network with two line circuits connected at both ends to the common buses. This scheme is obtained from the general scheme of Fig. 2.2, considering the following:

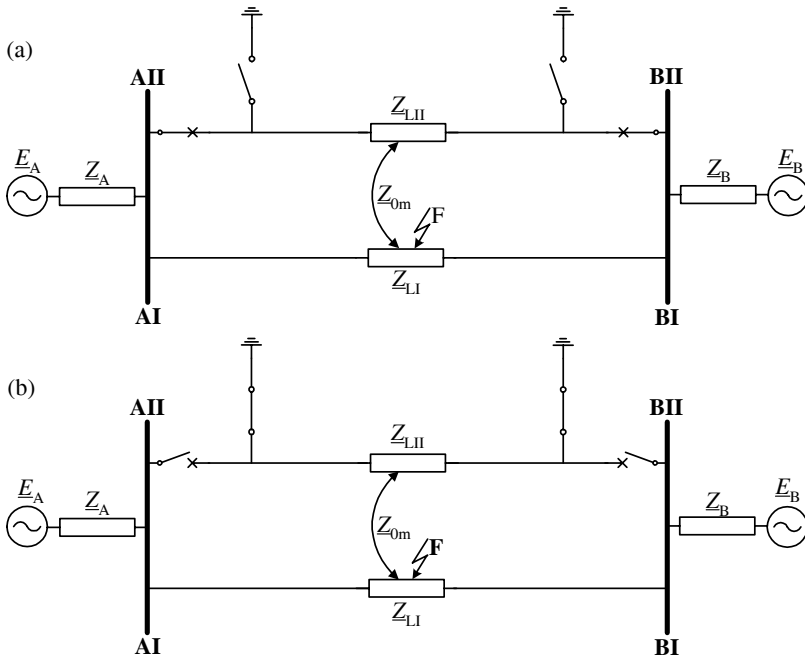
- equivalent source ( $\underline{E}_A$ ,  $\underline{Z}_A$ ) obtained as the resultant for parallel connection of the sources: ( $\underline{E}_{AI}$ ,  $\underline{Z}_{AI}$ ) and ( $\underline{E}_{AII}$ ,  $\underline{Z}_{AII}$ );
- equivalent source ( $\underline{E}_B$ ,  $\underline{Z}_B$ ) obtained as the resultant for parallel connection of the sources: ( $\underline{E}_{BI}$ ,  $\underline{Z}_{BI}$ ) and ( $\underline{E}_{BII}$ ,  $\underline{Z}_{BII}$ ); and
- extra link ( $\underline{Z}_F$ ) obtained as the resultant for parallel connection of the following impedances:  $\underline{Z}_{AI\_BI}$ ,  $\underline{Z}_{AI\_BII}$ ,  $\underline{Z}_{AII\_BI}$ ,  $\underline{Z}_{AII\_BII}$ .

The extra link shown in the network of Fig. 2.3 is not always present, especially in high-voltage networks that are not highly interconnected. Operating conditions of a double-circuit line could change due to different reasons, such as load dispatch, forced outage, scheduled maintenance, etc. The mutual coupling of double-circuit lines depends on the mode of operation of the healthy circuit ( $\underline{Z}_{LII}$ ), which is in parallel to the faulted-line circuit ( $\underline{Z}_{LI}$ ) considered. In order to present these modes, the status of circuit breakers and also grounding connectors of the healthy parallel line has to be considered [201].



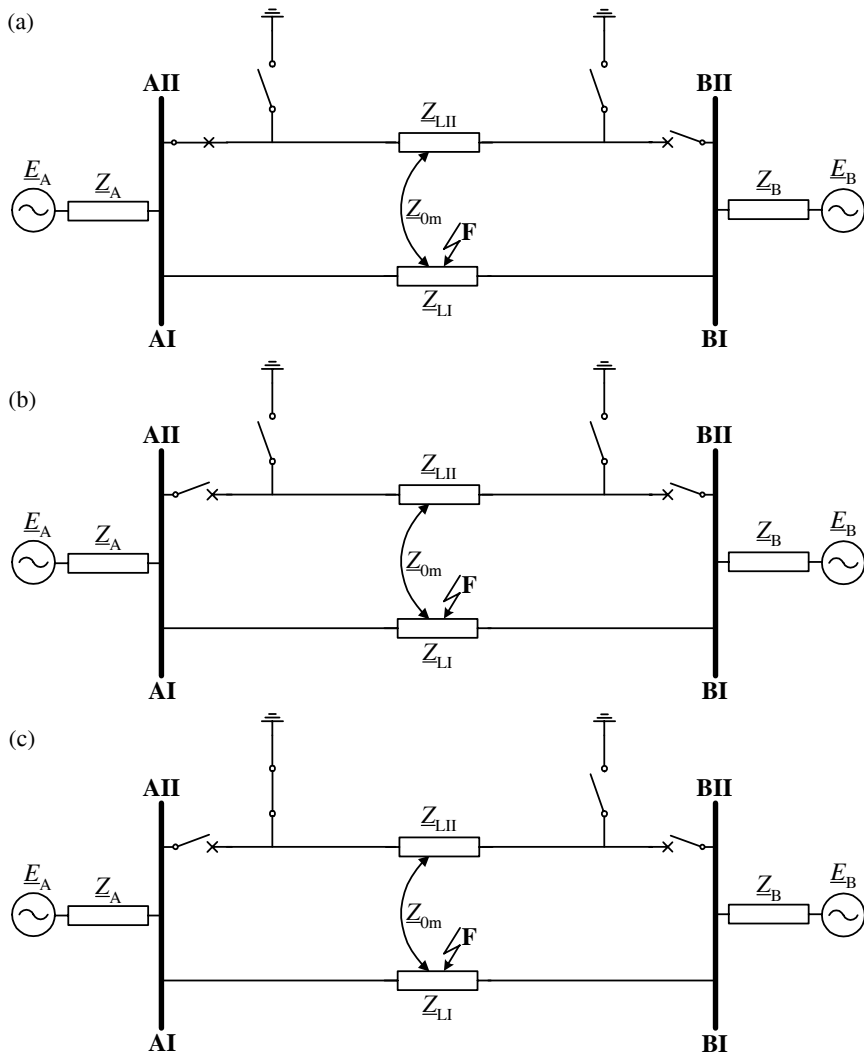
**Fig. 2.3** Schematic diagram of power network with double-circuit overhead line terminated at both ends at common buses

Figure 2.4 presents two modes for which the mutual coupling of parallel lines is of interest. In the case of Fig. 2.4a the parallel line is in operation, which is the normal operating mode. The mutual coupling of parallel lines also exists if the parallel line is switched off and grounded at both ends [114] (Fig. 2.4b).



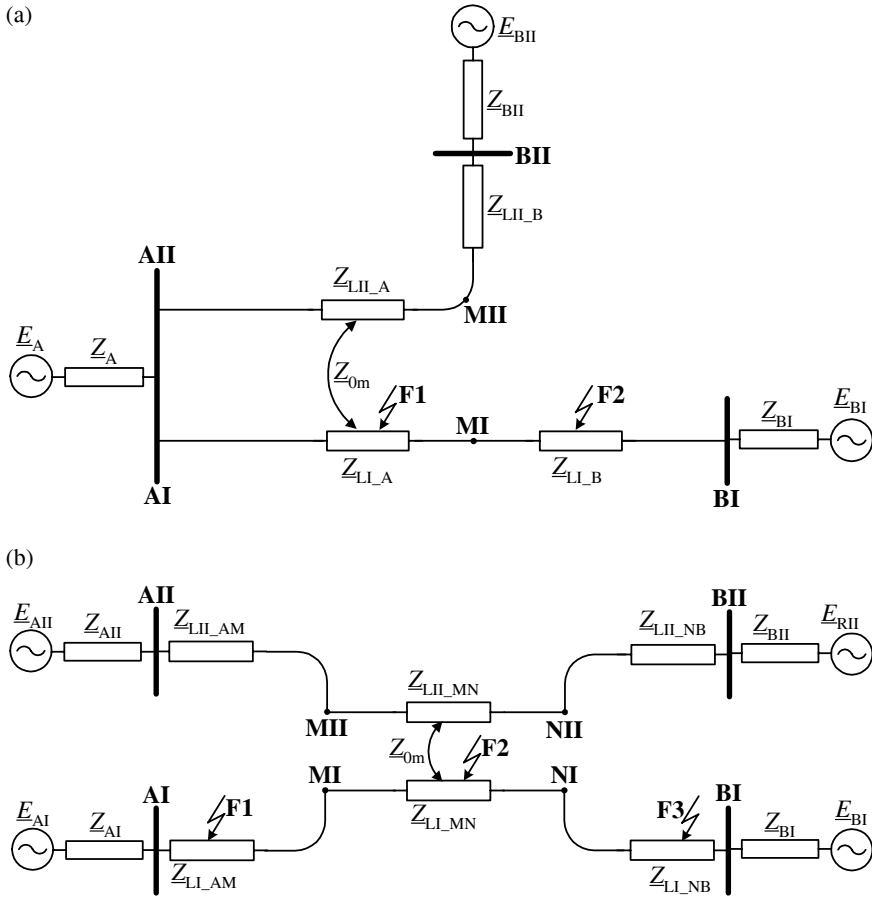
**Fig. 2.4** Double-circuit overhead-line modes with mutual coupling of parallel lines: (a) both lines in operation, and (b) parallel line is switched off and grounded at both ends

Figure 2.5 presents three cases for which there is a discontinuity for the current flow in the healthy parallel line, and therefore there is no mutual coupling between the lines.



**Fig. 2.5** Double-circuit overhead-line modes with no mutual coupling of parallel lines: (a) parallel line is switched off at one end (BII) and not grounded, (b) parallel line is switched off at both ends and not grounded, and (c) parallel line is switched off at both ends and grounded only at one end

In some cases [113, 350], the line circuits may run in parallel only for a part of the route. The circuits for this part are mutually coupled, while for the remaining part of the route, they are hung on different towers and are terminated at distant substations. This is illustrated in Fig. 2.6.



**Fig. 2.6** Examples of power networks containing partially parallel line circuits with mutual coupling for the line sections: (a)  $Z_{LI\_A}$ ,  $Z_{LII\_A}$ , and (b)  $Z_{LI\_MN}$ ,  $Z_{LII\_MN}$

Figure 2.6 presents two examples of power networks with partially parallel circuits. The need for taking into account the mutual coupling effect depends on the fault position: Fig. 2.6a – faults F1, F2; Fig. 2.6b – faults F1, F2, F3. Considering the fault loop between bus AI and fault point F1 in the network of Fig. 2.6a, the mutual coupling has to be taken into account along the whole distance. By contrast, as regards the fault loop between bus AI and the fault point F2, the mutual coupling has to be considered for the distance between bus AI and point MI, and not for the remaining part (MI–F2).

### 2.2.3 Multi-terminal and Tapped Lines

It is for economical or environmental-protection reasons that use is made of multi-terminal and tapped lines [350]. Lines having three or more terminals with substantial generation behind each are named multi-terminal lines [350]. Depending on the number of terminals we can distinguish three-terminal lines having three terminals, four-terminal lines having four terminals, and so on.

Tapped lines are those having three or more terminals with substantial power generation behind each, at a maximum at two of them [350]. The number of taps per line varies from one to even more than ten. The taps themselves feed only loads, which means that they are terminated by the passive networks, while at the remaining terminals there are active networks (with power generation) [81, 350].

Examples of power-network configurations with single-circuit three-terminal line are shown in Fig. 2.7. In the case of using double-circuit lines, typical configurations are as shown in Fig. 2.8.

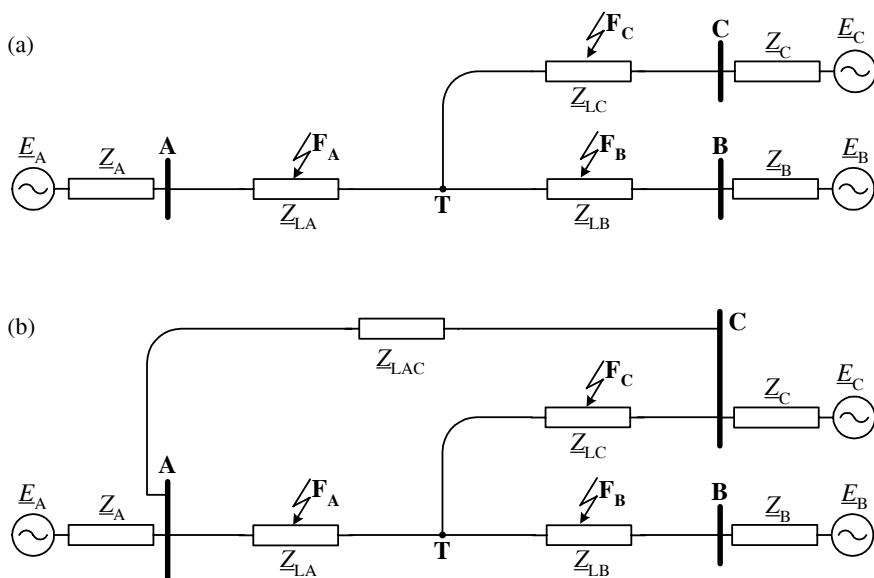


**Fig. 2.7** Examples of power-network configurations with single-circuit three-terminal line: (a) basic teed network, and (b) teed network with extra link between two substations



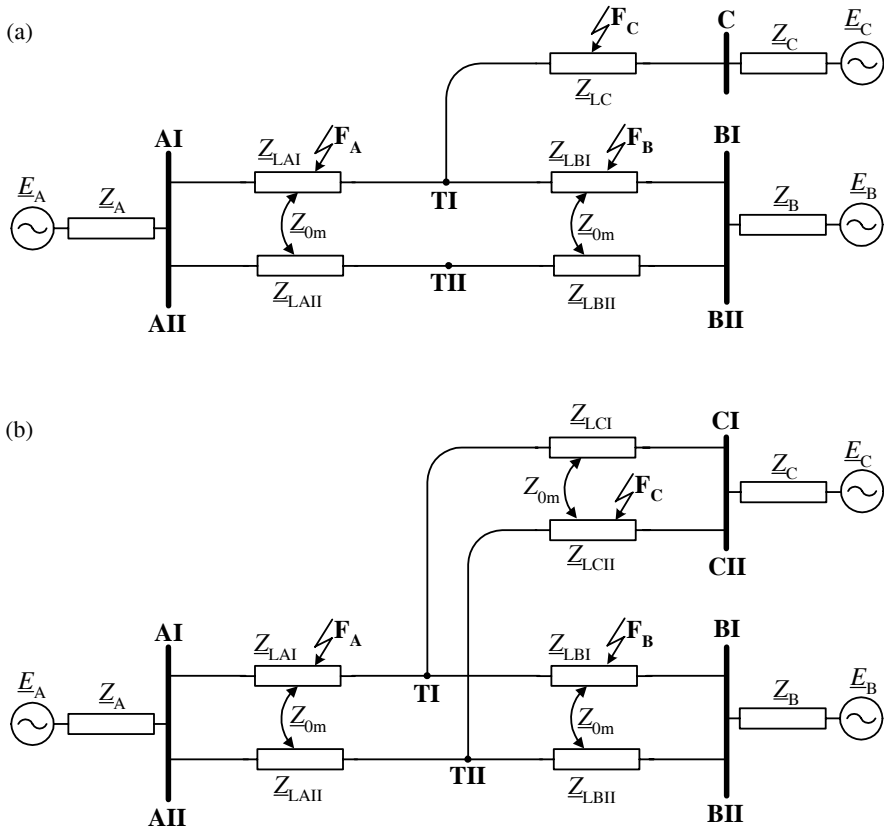


**Fig. 2.8** Examples of power-network configurations with parallel three-terminal line: (a) two line sections are of double-circuit type, and (b) all three line sections are double circuits

Figure 2.9 presents typical configurations of power networks with tapped line supplying load in two different ways [350]: via a transformer connected to the tap point through a circuit breaker (Fig. 2.9a) and additionally with overhead line section ( $Z_{LC}$ ), Fig. 2.9b.

Fault location on multi-terminal and tapped lines relies on determining the following:

- identifying the line section at which the fault ( $F_A$  or  $F_B$  or  $F_C$ ) occurred; and
- determining the distance to fault for the faulted section, usually measured from the respective bus (A, B or C) towards the fault point ( $F_A$  or  $F_B$  or  $F_C$ ).

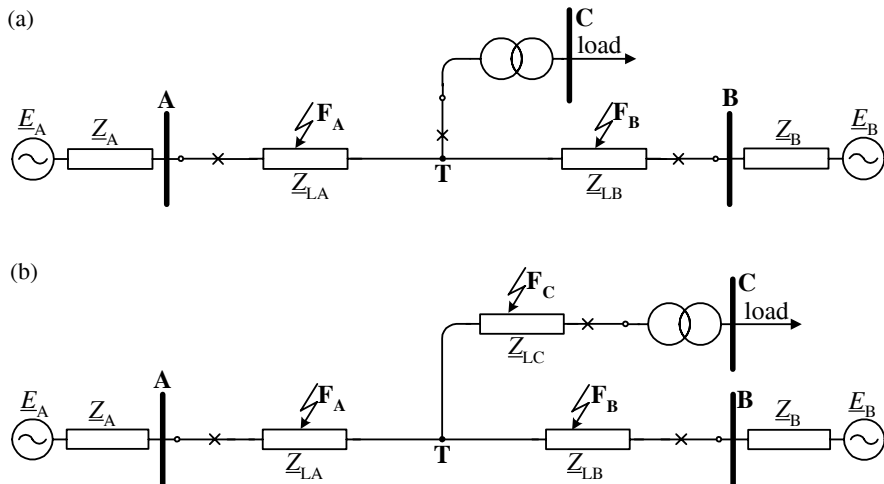


**Fig. 2.9** Typical configurations of power networks with tapped line supplying load through: (a) transformer, and (b) overhead line ( $Z_{LC}$ ) and transformer

### 2.2.4 Overhead Line and Cable Composite Networks

In Figs. 2.10 and 2.11, examples of configurations of overhead line and cable composite networks [214, 308] are presented.

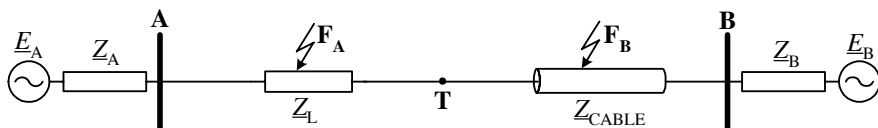


**Fig. 2.10** Overhead line in series connection with cable

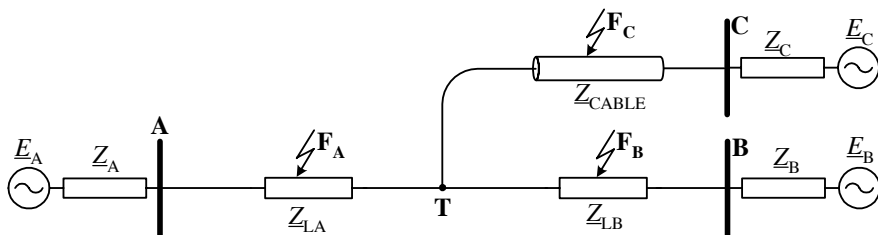


**Fig. 2.11** Overhead line tapped with cable

Fault location in such networks is considered to be a difficult task due to large differences in parameters of the line and cable. Moreover, the problem of cable

parameters changing, especially changes in its relative permittivity occurring with aging, has to be accounted for [308].

## 2.3 Models of Overhead Lines

Models of overhead lines are considered in strict relation to a particular application. Among different applications, the line models are considered in relation to the following:

- representing a faulted line in the fault-location algorithm; and
- simulating faults for generating the fault data, which is used in evaluation of the fault-location algorithms under study [56, 57, 203, 207].

In this section, the representation of a faulted line in fault-location algorithms is addressed. Assumption of the line model is a starting point for derivation of the fault-location algorithms.

In turn, the line models adopted in simulation of line faults are widely described in reference manuals (theory books) of the well-known simulation transients programs, such as ATP-EMTP [56] and others, and therefore are not considered here.

Overhead-line parameters are calculated using supporting routines available in the simulation programs. Also, an on-line measurement of transmission-line impedance performed either during normal operation or during faults is used in practice. In general, there are two types of line models:

- lumped-parameter models; and
- distributed-parameter models.

Lumped-parameter models represent a line by lumped elements, whose parameters are calculated at a single frequency, predominantly the fundamental power frequency. Using these models, steady-state calculations for fault location or transient simulations in the neighborhood of the frequency considered can be performed.

As opposed to the lumped-parameter models, the distributed-parameter line models are used for more accurate representation of the line. Two categories of distributed-parameter line models can be distinguished:

- constant-parameter model; and
- frequency-dependent parameter model.

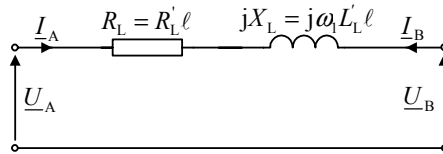
Series parameters: resistance ( $R$ ), inductance ( $L$ ), and shunt parameters: capacitance ( $C$ ) and conductance ( $G$ ) characterize the line. Usually, line conductance, which accounts for the leakage currents along the insulators and in the air, can be neglected, except at very low frequencies. Shunt capacitance can usually be assumed as frequency independent. In turn, series resistance and inductance can be

considered to be frequency dependent. However, this is considered for the simulation [56, 200] and rather not for representing a line in the fault-location algorithm.

### 2.3.1 Lumped-parameter Models

In the simplest lumped-parameter model of an overhead line, only the series resistance ( $R_L$ ) and reactance ( $X_L$ ) are included (Fig. 2.12). Such a model is considered adequate for representing a short line, usually less than 80 km long [84].

**Fig. 2.12** Model of short unfaulted overhead line



In Fig. 2.12, the following signals and parameters are used:

$\underline{U}_A, \underline{U}_B$  – voltage from A and B line ends,

$\underline{I}_A, \underline{I}_B$  – current from A and B line ends,

$R'_L, L'_L$  – line resistance and inductance per unit length,

$\ell$  – line length,

$\omega_1$  – angular fundamental frequency.

The circuit of Fig. 2.12 applies either to single-phase or completely transposed three-phase lines operating under balanced conditions. For a completely transposed three-phase line and balanced conditions, line resistance and inductance are considered for the positive-sequence. In turn,  $\underline{U}_A, \underline{U}_B$  are the positive-sequence line-to-neutral voltages;  $\underline{I}_A, \underline{I}_B$  are the positive-sequence line currents.

Under unbalanced conditions, mainly under faults, a three-phase line representation has to be considered. Figure 2.13 presents a faulted line together with the equivalent sources behind the line terminals A and B. A fault (occurring at a point marked by F) divides the line into two segments:

- A–F of the relative length  $d$  (p.u.),
- F–B of the relative length  $(1-d)$  (p.u.).

All signals (voltages and currents) in the circuit of Fig. 2.13 are three-phase (note that particular phases are marked in subscripts with letters: a, b, c), and thus are represented by  $3 \times 1$  column vectors, as for example, for the sending end voltage  $\underline{U}_A$  we have:

$$\underline{U}_A = \begin{bmatrix} \underline{U}_{Aa} \\ \underline{U}_{Ab} \\ \underline{U}_{Ac} \end{bmatrix} \quad (2.1)$$

All impedances are described by  $3 \times 3$  matrices, as for example, for the line impedance:

$$\mathbf{Z}_L = \begin{bmatrix} \underline{Z}_{Laa} & \underline{Z}_{Lab} & \underline{Z}_{Lac} \\ \underline{Z}_{Lba} & \underline{Z}_{Lbb} & \underline{Z}_{Lbc} \\ \underline{Z}_{Lca} & \underline{Z}_{Lcb} & \underline{Z}_{Lcc} \end{bmatrix} \quad (2.2)$$

where:

diagonal elements present the self-impedances of the phase conductors and off-diagonal elements present the mutual impedances between two phase conductors, for which the following is satisfied:  $\underline{Z}_{Lba} = \underline{Z}_{Lab}$ ,  $\underline{Z}_{Lca} = \underline{Z}_{Lac}$ ,  $\underline{Z}_{Lcb} = \underline{Z}_{Lbc}$ .

Note that the line in Fig. 2.13 is represented with only series parameters, while shunt parameters are here neglected.

At the fault point there is a three-phase fault model marked by  $\underline{Z}_F$ , while  $I_F$ ,  $\underline{U}_F$  denote the total fault current and voltage at the fault, respectively. Detailed considerations for the fault models are presented in Chap. 3.

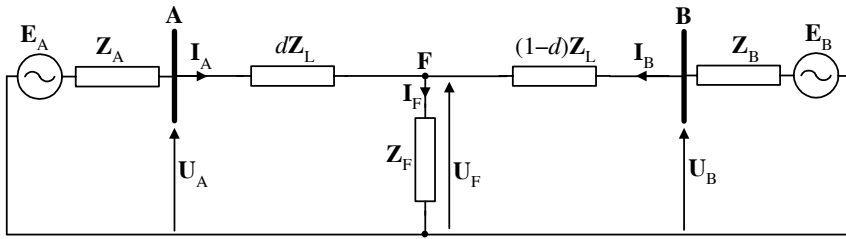
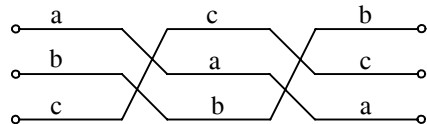


**Fig. 2.13** Circuit diagram of three-phase faulted line using matrices for presenting components (sources and impedances) and column matrices for signals

The self- and mutual impedances and admittances of each phase of overhead lines are determined by line geometry and they are not identical for all phases. In general, the line-impedance matrix  $\mathbf{Z}_L$  is not symmetrical. For a symmetrical impedance matrix the diagonal elements are equal and the off-diagonal elements are equal, too. This is satisfied if the line is completely transposed. A complete transposition (Fig. 2.14) is achieved by exchanging the conductor positions along the line in such a way that each phase (a, b and c) occupies each position for one-third of the line length.

**Fig. 2.14** Completely transposed section of three-phase line



For a completely transposed three-phase line the impedance matrix is symmetrical as follows:

$$\underline{\mathbf{Z}}_L = \begin{bmatrix} \underline{Z}_{Ls} & \underline{Z}_{Lm} & \underline{Z}_{Lm} \\ \underline{Z}_{Lm} & \underline{Z}_{Ls} & \underline{Z}_{Lm} \\ \underline{Z}_{Lm} & \underline{Z}_{Lm} & \underline{Z}_{Ls} \end{bmatrix} \quad (2.3)$$

where in the last position of the subscript for the matrix impedance elements the character of the impedance is denoted by s – self-impedance of the phase conductor and by m – mutual impedance between phase conductors.

If the transposition technique is not applied, the impedance matrix is no longer a symmetrical one; however, the following simplification is sometimes made. It relies on using the averaged value for the diagonal and the average for the off-diagonal elements. In this case, additional ramifications with respect to accuracy of the calculation results occur. Applying such simplification one gets:

$$\underline{Z}_{Ls} = \frac{1}{3}(\underline{Z}_{La a} + \underline{Z}_{Lb b} + \underline{Z}_{Lc c}) \quad (2.4)$$

$$\underline{Z}_{Lm} = \frac{1}{3}(\underline{Z}_{La b} + \underline{Z}_{Lb c} + \underline{Z}_{Lc a}) \quad (2.5)$$

As a result, one obtains a symmetrical impedance matrix (2.3), whose symmetry is of advantage; however, one must accept certain deterioration of accuracy.

Owing to the symmetry, it is possible to apply a method of symmetrical components, developed by C.L. Fortescue in 1918, which is known from numerous references. Based on this method, a linear transformation from phase components to a set of symmetrical components, as for example for the sending-end voltage  $\underline{U}_A$ , is performed according to:

$$\begin{bmatrix} \underline{U}_{A0} \\ \underline{U}_{A1} \\ \underline{U}_{A2} \end{bmatrix} = \frac{1}{3} \begin{bmatrix} 1 & 1 & 1 \\ 1 & \underline{a} & \underline{a}^2 \\ 1 & \underline{a}^2 & \underline{a} \end{bmatrix} \cdot \begin{bmatrix} \underline{U}_{Aa} \\ \underline{U}_{Ab} \\ \underline{U}_{Ac} \end{bmatrix} \quad (2.6)$$

where:

$\underline{U}_{Aa}$ ,  $\underline{U}_{Ab}$ ,  $\underline{U}_{Ac}$  – voltage from phases: a, b, c,

$\underline{U}_{A0}$ ,  $\underline{U}_{A1}$ ,  $\underline{U}_{A2}$  – zero-, positive- and negative-sequence voltage,

$\underline{a} = 1 \angle 120^\circ = -0.5 + j0.5\sqrt{3}$  is a complex number with unit magnitude and  $120^\circ$  phase angle.

Note that multiplying any phasor by  $\underline{a}$  results in rotating it by  $120^\circ$  counter-clockwise.

For the transformation (2.6) the sequence of phases: (a, b, c) is assumed to be the base, in which phase (a) is considered as the first one in this sequence. Sometimes it is convenient to apply the transformation from phase components into the symmetrical components, assuming the other sequences of phases: (b, c, a) or (c, a, b), in which the phase b or phase c starts the sequence, respectively.

Transformation from symmetrical components into the phase components is defined as follows:

$$\begin{bmatrix} \underline{U}_{Aa} \\ \underline{U}_{Ab} \\ \underline{U}_{Ac} \end{bmatrix} = \begin{bmatrix} 1 & 1 & 1 \\ 1 & \underline{a}^2 & \underline{a} \\ 1 & \underline{a} & \underline{a}^2 \end{bmatrix} \cdot \begin{bmatrix} \underline{U}_{A0} \\ \underline{U}_{A1} \\ \underline{U}_{A2} \end{bmatrix} \quad (2.7)$$

Use of the symmetrical-components method to a three-phase network, which is represented by the symmetrical impedance matrix, such as (2.3), allows this network to be decoupled into three sequence networks, which are simpler to analyze. These sequence networks are called the zero-sequence, positive-sequence and negative-sequence networks. The sequence networks results can then be superposed to obtain three-phase network results by using (2.7).

In the sequence networks, the line is represented by its respective sequence impedances:

- positive- and negative-sequence impedance, which are identical:

$$\underline{Z}_{1L} = \underline{Z}_{2L} = \underline{Z}_{Ls} - \underline{Z}_{Lm} \quad (2.8)$$

- zero-sequence impedance:

$$\underline{Z}_{0L} = \underline{Z}_{Ls} + 2\underline{Z}_{Lm} \quad (2.9)$$

Note that the positive- and negative-sequence impedances, as stated in (2.8), are equal. This is so for linear, symmetric impedances representing non-rotating power system items such as overhead lines and transformers.

Figure 2.15 presents models of a faulted single-circuit overhead line, together with the equivalent sources behind the line terminals, for the respective sequences. There are three circuits, which can be analyzed separately. These circuits can be composed into one resultant circuit by connecting them at points of unbalance and including the fault-path resistance  $R_F$ . At these points of unbalance, the respective sequence components of the total fault current ( $\underline{I}_{F1}$ ,  $\underline{I}_{F2}$ ,  $\underline{I}_{F0}$ ) flow into the sequence circuit, and flow out of the respective circuit. The particular sequence networks are connected in such a way as to satisfy the particular fault-type constraints.

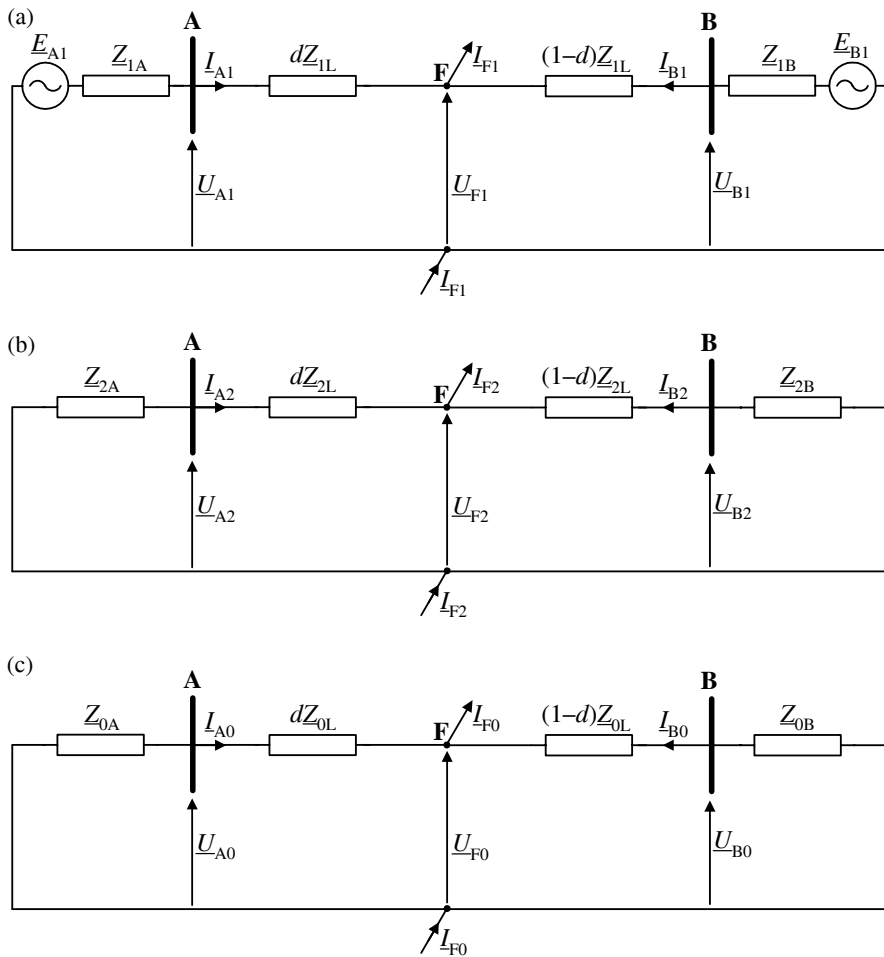


**Fig. 2.15** Equivalent networks of single-circuit faulted line for: (a) positive-sequence, (b) negative-sequence, and (c) zero-sequence

Figure 2.16 shows the connection of the sequence networks for a single phase-to-ground fault: a–g fault. The sequence networks are connected in series and additionally the triple fault resistance ( $3R_F$ ) is included. The series connection of Fig. 2.16 can also be applied for the remaining single phase-to-ground faults: b–g, c–g, however, this makes it necessary to use the following sequences of phases: (b, c, a) and (c, a, b), respectively.



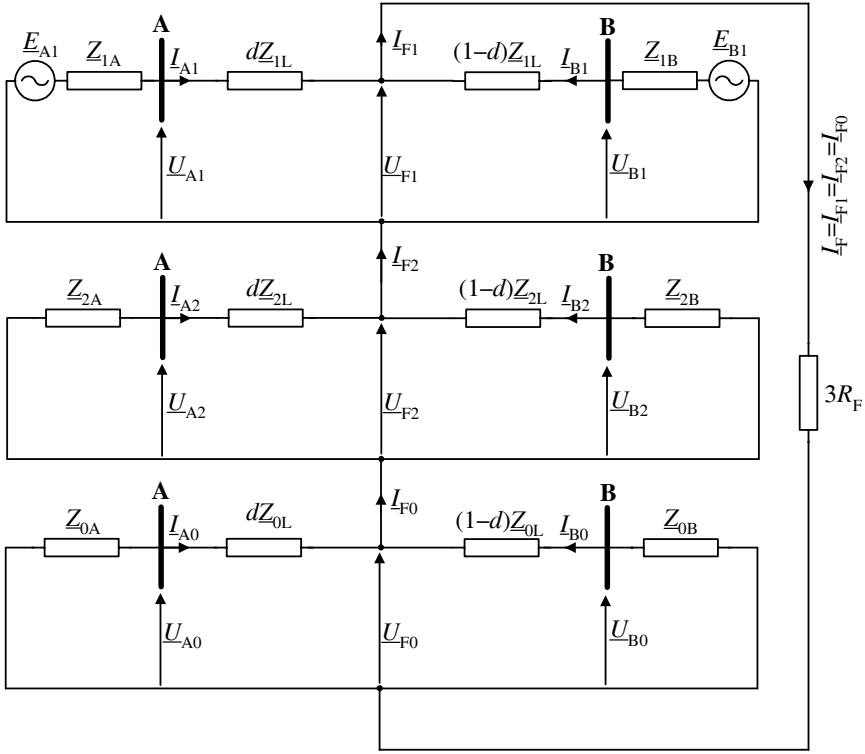


**Fig. 2.16** Connection of sequence networks for single phase-to-ground fault (a–g fault) involving fault resistance  $R_F$

In Fig. 2.17, equivalent circuit diagrams of a double-circuit line for the positive- and negative-sequence are shown.

In Fig. 2.18, equivalent circuits of a double-circuit line, with both circuits in operation [11, 109, 114, 122, 140, 286, 293, 345], for the zero-sequence are presented. As a result of mutual coupling of the line circuits, the current flowing in the faulted line AI–BI influences the voltage profile in the healthy parallel line AII–BII, and *vice versa*. In particular, in the faulted line (AI–BI) one can distinguish the following voltage drops (Fig. 2.18a):

- voltage drops resulting from the flow of the faulted-line current:

$$\underline{U}_0^A = d\underline{Z}_{0LI} \underline{I}_{A10} \quad (2.10)$$

$$\underline{U}_0^B = (1-d)\underline{Z}_{0LI} (\underline{I}_{A10} - \underline{I}_{F0}) \quad (2.11)$$

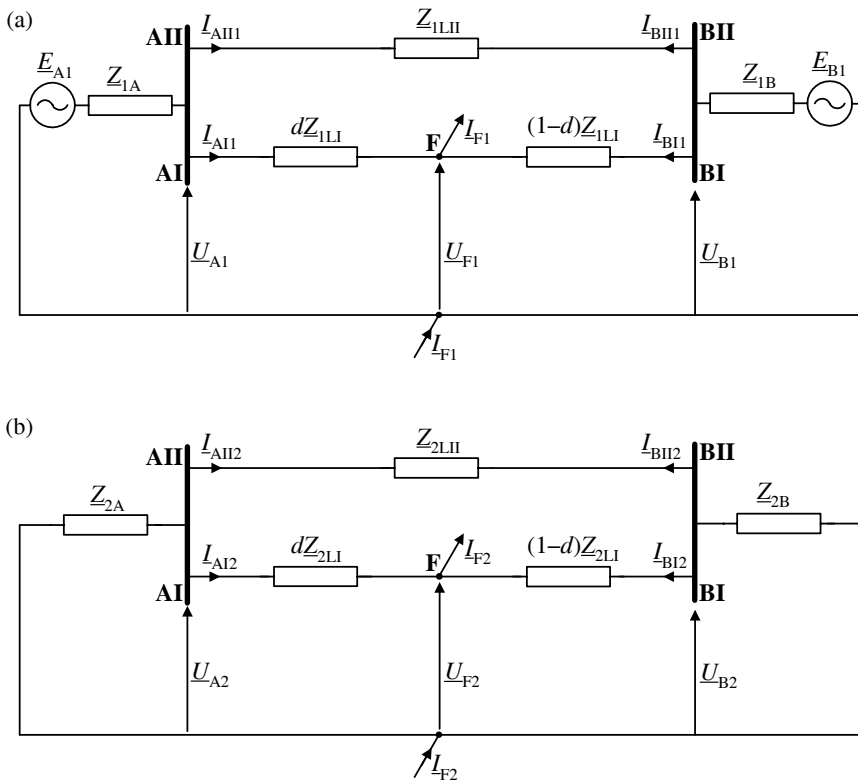


**Fig. 2.17** Equivalent networks of double-circuit faulted line for: (a) positive-sequence, and (b) negative-sequence

- voltage drops resulting from the flow of the current in the healthy parallel line:

$$\underline{U}_0^C = d \underline{Z}_{0m} \underline{I}_{AII0} \quad (2.12)$$

$$\underline{U}_0^D = (1-d) \underline{Z}_{0m} \underline{I}_{AII0} \quad (2.13)$$

In the healthy line (AII–BII) there are the following voltage drops (Fig. 2.18a):

- voltage drops resulting from the flow of the healthy line current:

$$\underline{U}_0^E = d \underline{Z}_{0LII} \underline{I}_{AII0} \quad (2.14)$$

$$\underline{U}_0^F = (1-d) \underline{Z}_{0LII} \underline{I}_{AII0} \quad (2.15)$$

- voltage drops resulting from the flow of the current from the faulted line:

$$\underline{U}_0^G = d\underline{Z}_{0m} \underline{I}_{A10} \quad (2.16)$$

$$\underline{U}_0^H = (1-d)\underline{Z}_{0m} (\underline{I}_{A10} - \underline{I}_{F0}) \quad (2.17)$$

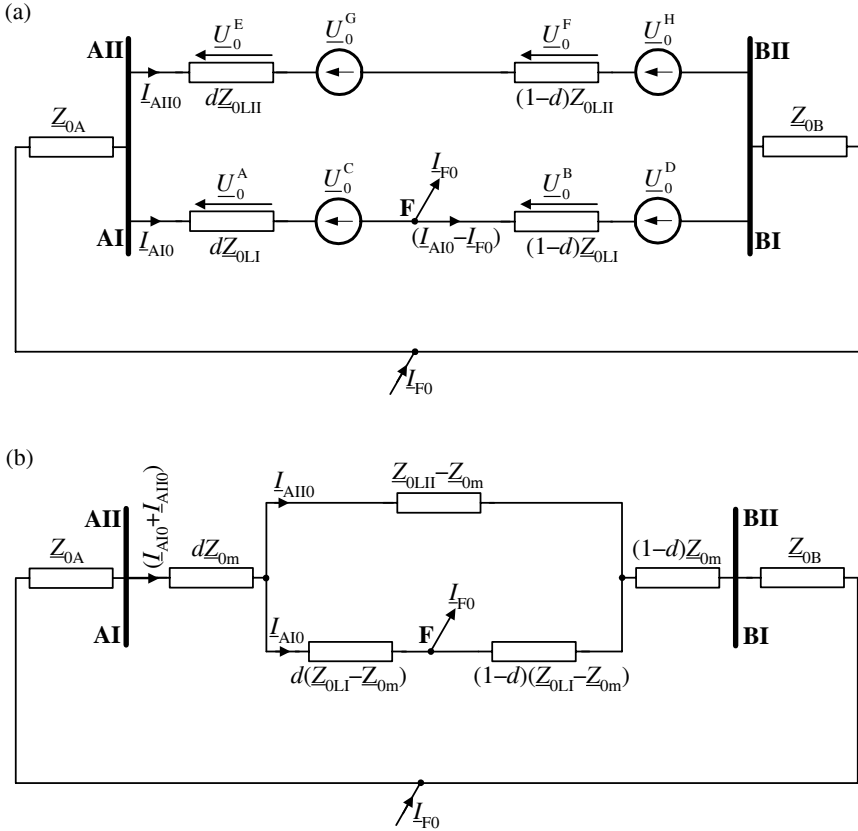


**Fig. 2.18** Equivalent networks of double-circuit faulted line with both lines in operation for zero-sequence: (a) general circuit, and (b) alternative circuit

The circuit of Fig. 2.18a can be transformed to the form shown in Fig. 2.18b, which is more convenient for use. For this purpose the voltage drop between the bus AI and fault point F is determined, taking into account (2.10) and (2.12):

$$\underline{U}_0^{(AI-F)} = d\underline{Z}_{0LI} \underline{I}_{A10} + d\underline{Z}_{0m} \underline{I}_{A10} \quad (2.18)$$

Adding and subtracting the term  $dZ_{0m} I_{A10}$  to the right-hand side of (2.18) leads to the following alternative form of (2.18):

$$\underline{U}_0^{(AI-F)} = d\underline{Z}_{0m} (\underline{I}_{A10} + \underline{I}_{AII0}) + d(\underline{Z}_{0LI} - \underline{Z}_{0m}) \underline{I}_{A10} \quad (2.19)$$

Analogously, after taking (2.11) and (2.13), one obtains for the voltage drop between the fault point F and the bus BI:

$$\underline{U}_0^{(F-BI)} = (1-d)(\underline{Z}_{0LI} - \underline{Z}_{0m})(\underline{I}_{A10} - \underline{I}_{F0}) + (1-d)\underline{Z}_{0m} (\underline{I}_{A10} + \underline{I}_{AII0} - \underline{I}_{F0}) \quad (2.20)$$

Similarly, for the healthy-line path (between buses AII, BII) one obtains:

$$\begin{aligned} \underline{U}_0^{(AII-BII)} &= d\underline{Z}_{0m} (\underline{I}_{A10} + \underline{I}_{AII0}) + (\underline{Z}_{0LII} - \underline{Z}_{0m}) \underline{I}_{AII0} \\ &\quad + (1-d)\underline{Z}_{0m} (\underline{I}_{A10} + \underline{I}_{AII0} - \underline{I}_{F0}) \end{aligned} \quad (2.21)$$

Taking into account (2.19)–(2.21), the circuit of Fig. 2.18b is obtained.

In Fig. 2.19, the mutual coupling effect is depicted for a double-circuit line with the healthy parallel line switched off and grounded at both ends [114].

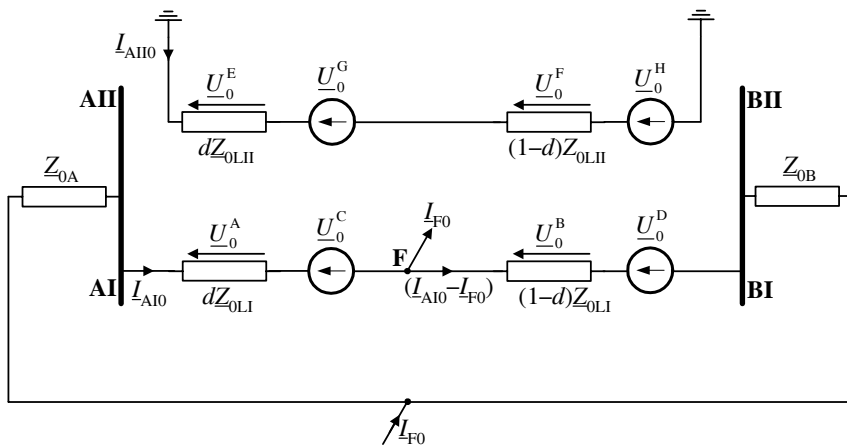


**Fig. 2.19** Zero-sequence equivalent network for double-circuit line with faulted line in operation and parallel healthy line switched off and grounded at both ends

The particular voltage drops for both lines are expressed in the same way as for the case of both lines in operation (2.14)–(2.17). The usual unavailability of the zero-sequence current from the healthy parallel line  $\underline{I}_{AII0}$  causes difficulty in reflecting the mutual coupling effect in the fault-location algorithms for this mode of operation. Therefore, it remains to estimate this current, based on other measurements available [114].

In the models presented so far (Figs. 2.12 and 2.13 and Figs. 2.15–2.19), only the series parameters of the line have been accounted for. These models can be used for short lines. For medium-length lines, typically ranging from 80 to 250 km, it is common to incorporate the shunt admittance to the line model [84]. Shunt conductance is usually neglected and only shunt capacitances of the line are considered for that. It is a common practice to lump the total shunt capacitance and insert half at each of the line sections. In this way the nominal  $\pi$  circuit is obtained [84].

Figure 2.20 shows a positive-sequence circuit of the faulted line, for which both sections (A–F and F–B) are represented using the nominal  $\pi$  circuits. The parameter  $\underline{Y}_{IL}$  used in describing admittances of shunt branches denotes:

$$\underline{Y}_{IL} = j\omega_1 C'_{IL} \ell \quad (2.22)$$

where:

- $C'_{IL}$  – line capacitance for the positive-sequence per unit length,
- $\ell$  – line length,
- $\omega_1$  – angular fundamental frequency.

The equivalent circuit diagrams for the remaining sequences are obtained analogously.

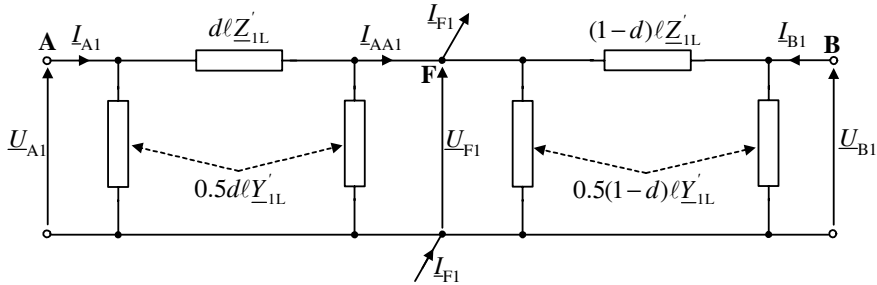


**Fig. 2.20** Equivalent circuit diagram of the network for the positive-sequence with the use of nominal  $\pi$  circuit for faulted line

Figure 2.21a presents a model of the line section between the bus A and the fault point F (as applied in Fig. 2.20). Note that a sought distance to fault ( $d$ ) is used for determining both the series impedance  $d\underline{Z}_{IL}$  and shunt admittance  $0.5d\underline{Y}_{IL}$ . However, it is inconvenient for performing fault-location calculations. In order to make the calculation simpler, the iterative calculations are usually performed in such a way that the unknown fault distance is left in the current iteration ( $n$ ) as related to the series impedance  $d_{(n)}\underline{Z}_{IL}$  (Fig. 2.21b). On the other hand, the shunt admittance is determined using the fault distance from the previous iteration ( $n-1$ ):  $0.5d_{(n-1)}\underline{Y}_{IL}$  at both ends of the faulted section (Fig. 2.21b). When starting the iterative calculations (iteration number:  $n = 1$ ) one takes the fault distance ob-

tained when neglecting the shunt admittance ( $\underline{Y}_{IL} = 0$ ) as the fault distance from the previous iteration (iteration number:  $n-1 = 0$ ).

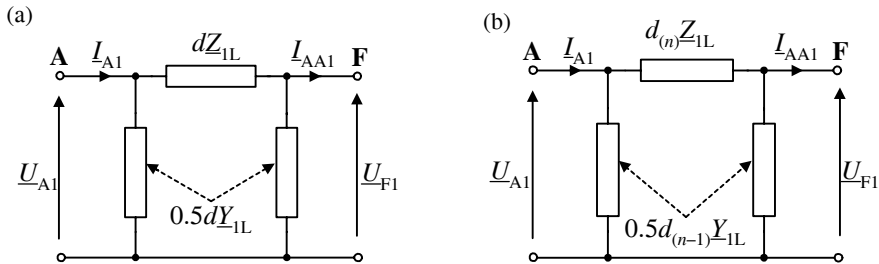


**Fig. 2.21** Model of faulted-line section from the side A for the positive-sequence: (a) basic model, and (b) model used in simple iterative fault-location calculations

### 2.3.2 Distributed-parameter Models

For short and medium-length lines using the lumped model is usually sufficient. In order to improve fault-location accuracy, especially in the case of long-length lines, the distributed nature of overhead-line parameters has to be considered.

In the distributed-parameter line models the voltage and current along the line are functions of the distance  $x$  (point X) from the sending end (A) of the line and the time  $t$  (Fig. 2.22). The voltage  $u(x, t)$  and current  $i(x, t)$  are related with the parameters of the line ( $R'_L, L'_L, C'_L$  – resistance, inductance and capacitance of the line per unit length) by the so-called *telegrapher's equations* [19, 88, 157]:

$$\frac{\partial u(x, t)}{\partial x} + L'_L \frac{\partial i(x, t)}{\partial t} = -R'_L i(x, t) \quad (2.23)$$

$$C'_L \frac{\partial u(x, t)}{\partial t} + \frac{\partial i(x, t)}{\partial x} = 0 \quad (2.24)$$

Note that in (2.24) the line conductance is neglected, which is a common practice.

Partial differential equations (2.23) and (2.24) can be solved using the method of characteristics developed by Collatz [37]. For this purpose the *modified telegrapher's equations* are formulated:

$$\frac{\partial v(x, t)}{\partial x} - \chi^2 \frac{\partial i(x, t)}{\partial t} = -\eta i(x, t) \quad (2.25)$$

$$\frac{\partial v(x, t)}{\partial t} - \frac{\partial i(x, t)}{\partial x} = 0 \quad (2.26)$$

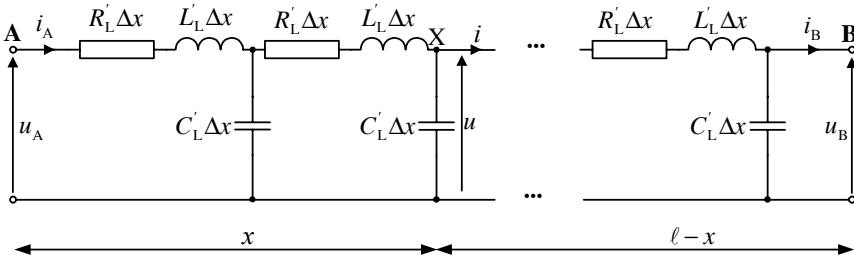


**Fig. 2.22** Distributed-parameter model of long overhead line

where:

$$v(x, t) = -C'_L u(x, t),$$

$$\chi = \sqrt{L'_L C'_L},$$

$$\eta = R'_L C'_L.$$

The traveling-waves method is applied as the alternative to solving the partial differential equations (2.25) and (2.26). In this method, the voltage and current are considered as two components: the forward and backward traveling waves [157].

A distributed-parameter model of an overhead line can also be applied for phasors. In this case, the so-called equivalent  $\pi$  circuit [84] is utilized. In Fig. 2.23, two such circuits are used for representing both line sections A–F and F–B. The model of Fig. 2.23 is for the general case, i.e., for the  $i$ th symmetrical component, where:  $i = 1$  – positive-sequence,  $i = 2$  – negative-sequence,  $i = 0$  – zero-sequence.

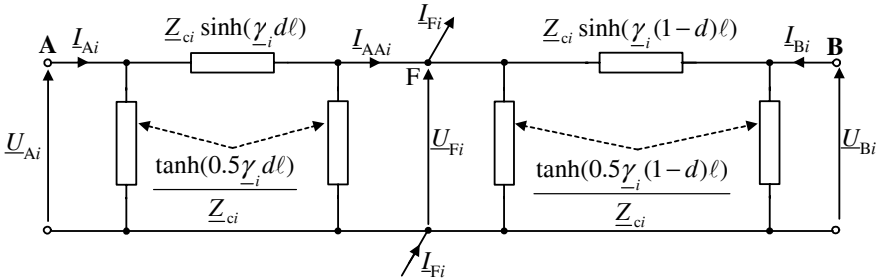


**Fig. 2.23** Distributed-parameter model of faulted line for the  $i$ th symmetrical component

In Fig. 2.23, both the series and shunt parameters of the line are distributed parameters and are expressed using:

- surge impedance of the line for the  $i$ th sequence:

$$\underline{Z}_{ci} = \sqrt{\frac{\underline{Z}'_{iL}}{\underline{Y}'_{iL}}} \quad (2.27)$$

- propagation constant of the line for the  $i$ th sequence:

$$\underline{\gamma}_i = \sqrt{\underline{Z}'_{iL} \underline{Y}'_{iL}} \quad (2.28)$$

Using the equivalent  $\pi$  circuit model, the voltage and current, for example, from the end A can be analytically transferred to the fault point F (Fig. 2.23) according to:

$$\underline{U}_{Fi} = \cosh(\underline{\gamma}_i d \ell) \underline{U}_{Ai} - \underline{Z}_{ci} \sinh(\underline{\gamma}_i d \ell) \underline{I}_{Ai} \quad (2.29)$$

$$\underline{I}_{Aai} = -\frac{1}{\underline{Z}_{ci}} \sinh(\underline{\gamma}_i d \ell) \underline{U}_{Ai} + \cosh(\underline{\gamma}_i d \ell) \underline{I}_{Ai} \quad (2.30)$$

An alternative representation of the faulted line, based on the distributed-parameter line model is depicted in Fig. 2.24 [84]. Both the series impedances and shunt admittances are expressed as the lumped parameter multiplied by the respective correction factor:

- correction factors for series impedances:

$$\underline{A}_i^{\text{sh}} = \frac{\sinh(\underline{\gamma}_i d \ell)}{\underline{\gamma}_i d \ell} \quad (2.31)$$

$$\underline{B}_i^{\text{sh}} = \frac{\sinh(\underline{\gamma}_i (1-d) \ell)}{\underline{\gamma}_i (1-d) \ell} \quad (2.32)$$

- correction factors for shunt admittances:

$$\underline{A}_i^{\text{th}} = \frac{\tanh(0.5 \underline{\gamma}_i d \ell)}{0.5 \underline{\gamma}_i d \ell} \quad (2.33)$$

$$\underline{B}_i^{\text{th}} = \frac{\tanh(0.5 \underline{\gamma}_i (1-d) \ell)}{0.5 \underline{\gamma}_i (1-d) \ell} \quad (2.34)$$

Using the correction factors (2.31)–(2.34) allows us to recalculate the lumped parameters into the distributed ones.



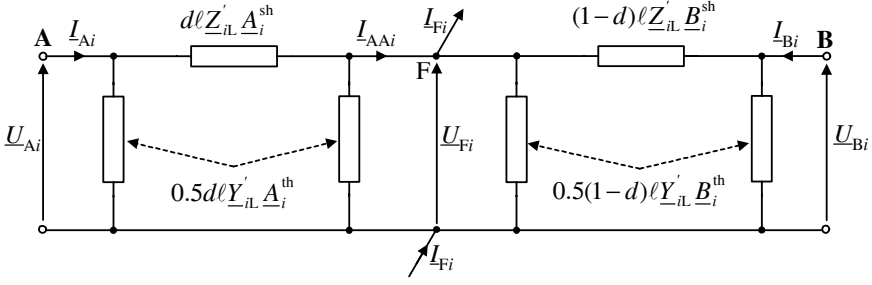


**Fig. 2.24** Distributed-parameter model of faulted line for the  $i$ th symmetrical component, with use of the correction factors for representing series and shunt parameters

In Fig. 2.25, the distributed-parameter model of a faulted line for the  $i$ th symmetrical component for application to simplified iterative fault-location calculations is presented.

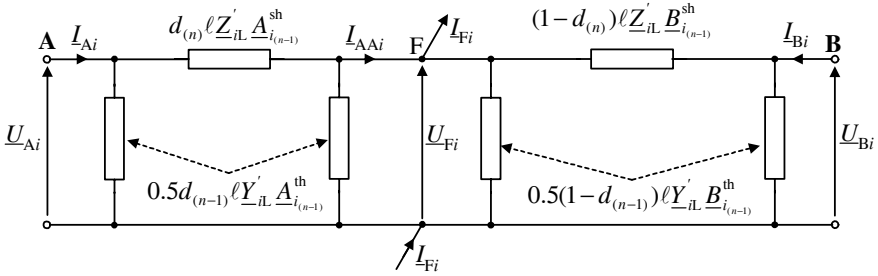


**Fig. 2.25** Distributed-parameter model of faulted line for the  $i$ th symmetrical component for application to simplified iterative calculations of fault location

The model of Fig. 2.25 is simpler in comparison to the strict model of Fig. 2.24. The unknown fault distance in the model of Fig. 2.25, which is calculated in the current iteration (iteration number:  $n$ ):  $d_{(n)}$ , is involved only to represent the series impedances. The shunt parameters are represented by the fault-distance value obtained in the previous iteration:  $d_{(n-1)}$ . Also, this value of fault distance is used for calculating all correction factors:

$$\underline{A}_{i(n-1)}^{sh} = \frac{\sinh(\gamma_i d_{(n-1)} \ell)}{\gamma_i d_{(n-1)} \ell} \quad (2.35)$$

$$\underline{B}_{i(n-1)}^{sh} = \frac{\sinh(\gamma_i (1 - d_{(n-1)}) \ell)}{\gamma_i (1 - d_{(n-1)}) \ell} \quad (2.36)$$

$$\underline{A}_{i(n-1)}^{\text{th}} = \frac{\tanh(0.5\underline{\gamma}_i d_{(n-1)} \ell)}{0.5\underline{\gamma}_i d_{(n-1)} \ell} \quad (2.37)$$

$$\underline{B}_{i(n-1)}^{\text{th}} = \frac{\tanh(0.5\underline{\gamma}_i (1 - d_{(n-1)}) \ell)}{0.5\underline{\gamma}_i (1 - d_{(n-1)}) \ell} \quad (2.38)$$

### 2.3.3 Modal Transformation

The symmetrical components approach was used in the preceding sections for presenting different line models. Yet, there is another technique based on modal transformation that considers the general case of an untransposed line [56].

Using the modal transformation [56, 135] the line-impedance matrix  $\mathbf{Z}$  and admittance matrix  $\mathbf{Y}$  are transformed into the matrices  $\mathbf{Z}_{\text{mode}}$ ,  $\mathbf{Y}_{\text{mode}}$ :

$$\mathbf{Z}_{\text{mode}} = \mathbf{T}_u^{-1} \mathbf{Z} \mathbf{T}_i \quad (2.39)$$

$$\mathbf{Y}_{\text{mode}} = \mathbf{T}_i^{-1} \mathbf{Y} \mathbf{T}_u \quad (2.40)$$

where the superscript  $(-1)$  denotes the matrix inversion.

The transformation (2.39) and (2.40) is performed in such a way that the matrices  $\mathbf{Z}_{\text{mode}}$ ,  $\mathbf{Y}_{\text{mode}}$  are diagonal, which means that the three-phase coupled network becomes decoupled into three decoupled single-phase networks.

Three-phase voltage  $\mathbf{U}$  and current  $\mathbf{I}$  vectors are transformed into the modal vectors  $\mathbf{U}_{\text{mode}}$ ,  $\mathbf{I}_{\text{mode}}$ . This is performed using the matrices  $\mathbf{T}_i$ ,  $\mathbf{T}_u$  (used in (2.39) and (2.40)):

$$\mathbf{U}_{\text{mode}} = \mathbf{T}_u^{-1} \mathbf{U} \quad (2.41)$$

$$\mathbf{I}_{\text{mode}} = \mathbf{T}_i^{-1} \mathbf{I} \quad (2.42)$$

For balanced (equally transposed) three-phase lines, both matrices  $\mathbf{T}_i$ ,  $\mathbf{T}_u$  are identical and are composed of the different real-value elements such as:

- Clarke transformation (also called the  $\alpha$ - $\beta$  transform) [25]:

$$\mathbf{T}_u = \mathbf{T}_i = \begin{bmatrix} 1 & 1 & 0 \\ 1 & -\frac{1}{2} & \frac{\sqrt{3}}{2} \\ 1 & -\frac{1}{2} & -\frac{\sqrt{3}}{2} \end{bmatrix} \quad (2.43)$$

$$\mathbf{T}_u^{-1} = \mathbf{T}_i^{-1} = \frac{1}{3} \begin{bmatrix} 1 & 1 & 1 \\ 2 & -1 & -1 \\ 0 & \sqrt{3} & -\sqrt{3} \end{bmatrix} \quad (2.44)$$

- Karrenbauer transformation:

$$\mathbf{T}_u = \mathbf{T}_i = \begin{bmatrix} 1 & 1 & 1 \\ 1 & -2 & 1 \\ 1 & 1 & -2 \end{bmatrix} \quad (2.45)$$

$$\mathbf{T}_u^{-1} = \mathbf{T}_i^{-1} = \frac{1}{3} \begin{bmatrix} 1 & 1 & 1 \\ 1 & -1 & 0 \\ 1 & 0 & -1 \end{bmatrix} \quad (2.46)$$

- Wedepohl transformation:

$$\mathbf{T}_u = \mathbf{T}_i = \begin{bmatrix} 1 & 1 & 1 \\ 1 & 0 & -2 \\ 1 & -1 & 1 \end{bmatrix} \quad (2.47)$$

$$\mathbf{T}_u^{-1} = \mathbf{T}_i^{-1} = \frac{1}{3} \begin{bmatrix} 1 & 1 & 1 \\ \frac{3}{2} & 0 & -\frac{3}{2} \\ \frac{1}{2} & -1 & \frac{1}{2} \end{bmatrix} \quad (2.48)$$

In the case of untransposed lines, there is also a possibility of determining the transformation matrices:  $\mathbf{T}_u$ ,  $\mathbf{T}_i$ , which are not identical. They can be applied for transforming the coupled phase quantities to decoupled modal quantities based on eigenvalue/eigenvector theory [135].

## 2.4 Series-compensated Lines

Power ( $P$ ) transfer capability of a traditional uncompensated transmission line (Fig. 2.1) is determined by the well-known formula (with line resistance and capacitance being neglected):

$$P = \frac{|\underline{U}_A| \cdot |\underline{U}_B|}{X_L} \sin(\delta) \quad (2.49)$$

where:

$\underline{U}_A, \underline{U}_B$  – phasors of voltage from the end A and B, respectively,

$X_L$  – line reactance,

$\delta$  – electric angle between the terminal voltage phasors.

The maximum value of  $\delta$  is limited by the stability constraints, and thus an increase in the power-transfer capability can be obtained by reducing the line reactance. This can be done by adding series-compensating capacitors to counteract series inductance. As a result, the total reactance of the series compensated line ( $X_{\text{total}}$ ) is equal to:

$$X_{\text{total}} = X_L - X_C \quad (2.50)$$

where  $X_C$  is the capacitor reactance.

The compensation degree is expressed by the following ratio:

$$k_{\text{SC}} = \frac{X_C}{X_L} 100\% \quad (2.51)$$

and usually falls within the range of 50 up to 90%.

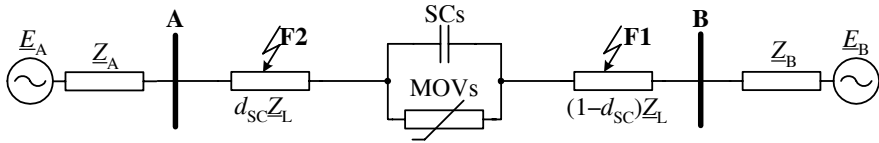
The capacitor compensation in high-voltage transmission networks is performed by adding series capacitors of the fixed value or of the value controlled with the thyristor circuits.

Use of the series capacitors besides increasing the power-transfer capability brings about several advantages to power-system operation [350], such as:

- improving power-system stability;
- reduced transmission losses;
- enhanced voltage control; and
- flexible power-flow control.

The environmental concerns are also of importance here since instead of constructing a new line, the power-transfer capability of the existing line is increased. The cost of introducing the series capacitor compensation is much lower than that of constructing a new equivalent overhead power line [350].

Usually, only one three-phase capacitor bank is installed on a power transmission line. As far as a single line is concerned, the one-line circuit diagram of the series-compensated line is as presented in Fig. 2.26. Series capacitors (SCs) are installed on the line at a distance  $d_{SC}$  (p.u.) from the bus A. In order to protect SCs against overvoltages they are equipped with MOVs. The SC and its MOV are the main components of the compensating bank installed in each phase of the line. Therefore, for the sake of simplifying the series-compensated transmission networks presented, only these components are indicated in the schemes (Fig. 2.26, Fig. 2.27 and further figures showing configurations of series-compensated networks).



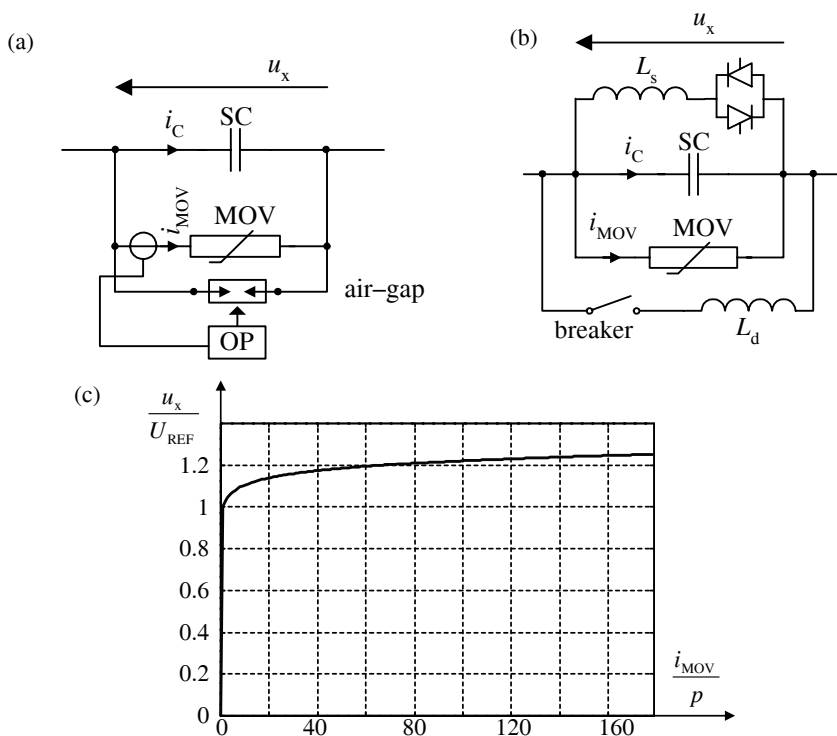
**Fig. 2.26** Single transmission line compensated with SCs and MOVs installed at midpoint

Figure 2.27a presents a scheme of the compensating bank from one phase of a line, which contains a fixed series capacitor [159, 194, 268]. Besides the SC and MOV there is a protection of MOV against overheating. This thermal (overload) protection (OP) measures the current conducted by the MOV. If the energy absorbed by the MOV exceeds its pre-defined limit the MOV becomes shunted by firing the air gap. Figure 2.27b presents a compensating bank with thyristor controlled capacitor [32, 46, 149, 340]. MOVs are non-linear resistors commonly approximated by the standard exponential formula:

$$\frac{i_{\text{MOV}}}{p} = \left( \frac{u_x}{U_{\text{REF}}} \right)^q \quad (2.52)$$

Figure 2.27c shows the voltage–current characteristic for the following parameters of the approximation (2.52):  $q = 23$ ,  $p = 1 \text{ kA}$ ,  $U_{\text{REF}} = 150 \text{ kV}$ .

Series capacitors equipped with MOVs, when set on a transmission line, create certain problems for its protective relays [61, 74, 75, 83, 91, 126, 146, 150, 159, 210, 227, 241, 251, 252, 267, 277, 282, 287] and fault locators [10, 64, 106, 111, 222, 228, 254, 264, 268, 272, 274, 276, 279, 284, 285, 340]. Under faults behind the SCs and MOVs (fault F1 in Fig. 2.19), a fault loop seen from the bus A becomes strongly non-linear, and as a consequence, the nature of transients as well as the steady-state situation are entirely different, compared with traditional uncompensated lines. In the case of faults in front of the SCs and MOVs (fault F2 in Fig. 2.26) the SCs and MOVs are outside the fault loop seen from the bus A; however, they influence the infeed of the fault from the remote substation B.



**Fig. 2.27** Series capacitor bank: (a) scheme of bank with fixed capacitor, (b) scheme of bank with thyristor-controlled capacitor, and (c) typical voltage–current characteristic of MOV

Adequate representation of the SCs and MOVs has to be applied for both protective relays and fault location. The form of this representation depends on the type of protection and fault-location algorithms. If these algorithms are based on the phasor technique, then the SCs and MOVs from a particular phase can be represented with the fundamental-frequency equivalent [86, 106, 111, 272, 274, 276, 284, 285] in the form of resistance–capacitive reactance series branch with parameters dependent on an amplitude of the current (fundamental-frequency component) measured in the phase of interest. When considering protection and fault-location algorithms based on a differential equation approach, the SC and MOV from a particular phase is represented with use of the estimated instantaneous voltage drop across the compensating bank [10, 74, 75, 268, 277, 282].

Figure 2.28 shows operation of SCs and MOVs under the sample fault on a 400-kV, 300-km transmission line compensated at  $k_{SC} = 80\%$ . The parameters of the approximation (2.52) are as taken for plotting the voltage–current characteristic from Fig. 2.27c. A single phase-to-ground fault (a–g fault) with fault resistance of  $10\ \Omega$  was applied just behind the SCs and MOVs. In Fig. 2.28a, the three-phase currents entering the SCs and MOVs are shown. The voltage drops across the SCs and MOVs are shown in Fig. 2.28b.

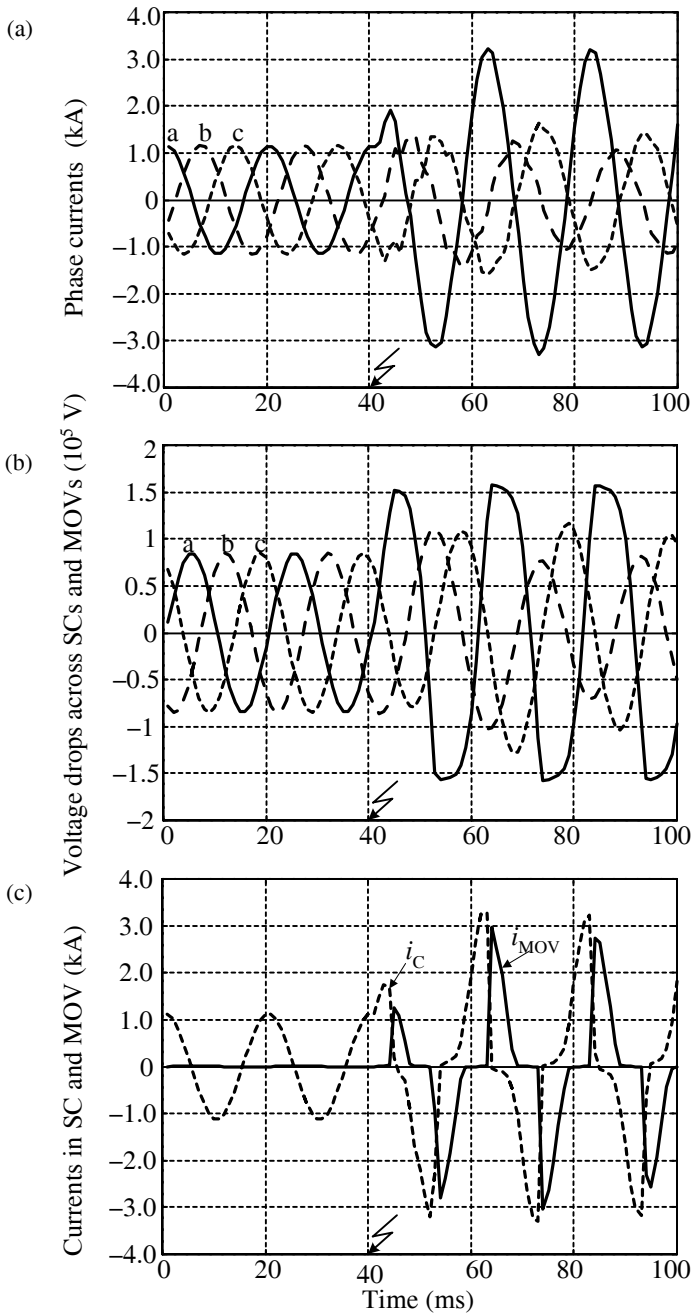
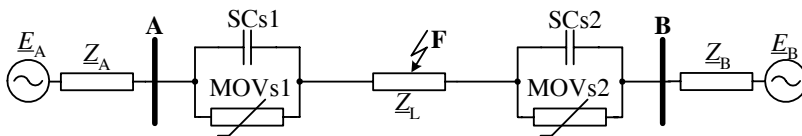


**Fig. 2.28** Operation of SCs and MOVs under the sample a-g fault: (a) phase currents entering SCs and MOVs, (b) voltage drops across SCs and MOVs, and (c) currents flowing in SC ( $i_C$ ) and in MOV ( $i_{MOV}$ ) from the faulted phase

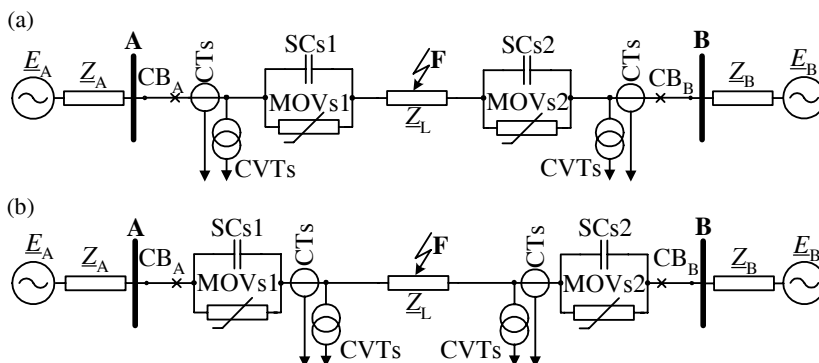
It can be observed that the voltage drop in the faulted phase (a) is limited to around  $\pm 150$  kV. Such a limitation results from applying the MOVs with the reference voltage:  $V_{REF} = 150$  kV. The waveforms of the voltage drop from the healthy phases (b, c) are distorted by sub-synchronous resonance oscillations. Such oscillations appear since MOVs from these phases operate in the linear range, conducting low current. The sub-synchronous resonance oscillations are also visible in currents entering the SCs and MOVs from the healthy phases (Fig. 2.28a).

Figure 2.28c shows division of the fault current from the faulted phase (a) into the parallel branches of the SC and its MOV. The SC and MOV conduct the fault current alternately, around for the quarter of the fundamental period. Such voltage limitation results from applying the MOVs with the reference voltage:  $V_{REF} = 150$  kV. The waveforms of the voltage drop from the healthy phases (b, c) are distorted by sub-synchronous resonance oscillations. Such oscillations appear since MOVs from these phases operate in the linear range, conducting low current. The sub-synchronous resonance oscillations are also visible in currents entering the SCs and MOVs from the healthy phases (Fig. 2.28a). Figure 2.28c shows division of the fault current from the faulted phase (a) into the parallel branches of the SC and its MOV. The SC and MOV conduct the fault current alternately, around for a quarter of the fundamental period.

Figure 2.29 depicts series capacitors compensation of the transmission line using the compensation banks installed at both ends [272, 350].



**Fig. 2.29** Transmission line compensated with SCs and MOVs banks at both ends



**Fig. 2.30** Placement of instrument transformers in the case of double-end series compensation: (a) on the bus side, and (b) on the line side



In the case of such compensation, the placement of current and voltage instrument transformers (CTs – current transformers, CVTs – capacitive voltage transformers) at the line ends is important for considering fault location. The instrument transformers can be placed on the bus side (Fig. 2.30a) or on the line side (Fig. 2.30b) [350].

Similarly, double-circuit transmission lines, analogously to the single line, can be compensated using the capacitor compensating banks installed at the midpoint in both circuits [279, 284, 285] (Fig. 2.31) or at the line ends (Fig. 2.32).

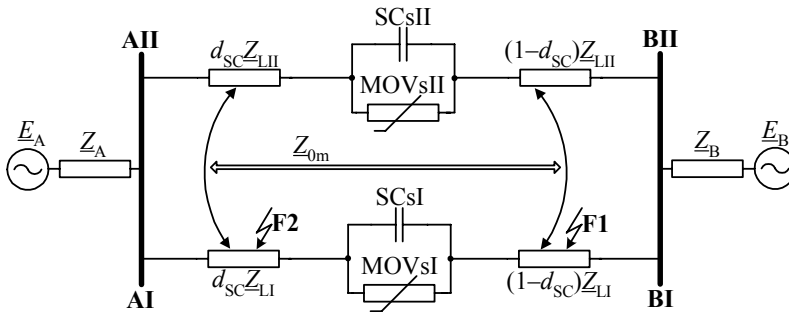


**Fig. 2.31** Double-circuit transmission lines with capacitor compensating banks installed at the midpoint in both circuits

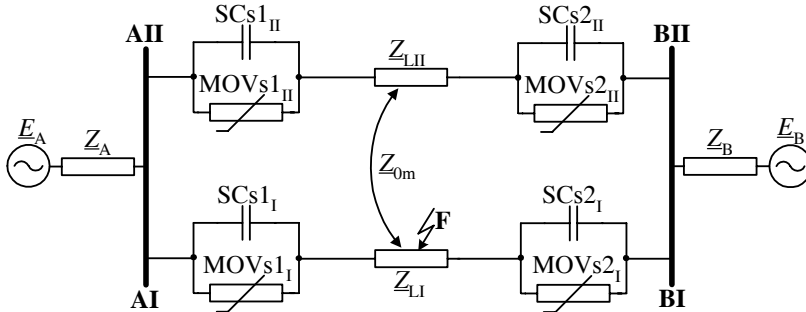


**Fig. 2.32** Double-circuit transmission lines with capacitor compensating banks installed at two ends in both circuits

## 2.5 Distribution Networks

### 2.5.1 Basic Principles of Distribution Systems

Distribution systems, also called medium voltage (MV) systems deliver the electrical energy to final step-down transformers at voltages below 132 kV (this value

may be different in particular systems). The MV networks provide supplies direct to large customers, but the vast majority of consumers are connected at low voltage via distribution transformers (MV/LV) [73, 87, 327]

A scheme of a typical distribution system is presented in Fig. 2.33. The MV networks are supplied from HV/MV-transforming substations. The electrical energy is then transported via a series of underground-cable and overhead-line circuits to the customers. In some cases a dispersed generation (DG) can be connected to the network. The particular line sections are of length from a few hundred meters to some dozens of kilometers. The distribution voltages in a specific service territory are likely similar because it is easier and more cost effective to stock spare parts when the system voltages are consistent. Although due to different loads and the network development, separate feeders are made up of sections with different technical data: varying cable cross-sections and overhead-line parameters.

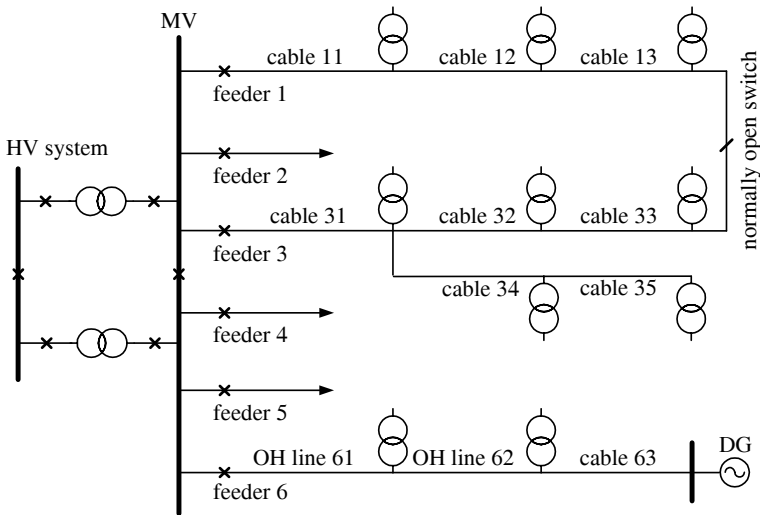


**Fig. 2.33** Typical configurations of MV network

The configuration layout and complexity of distribution networks vary widely depending on the application. From that point of view one can specify: rural systems; suburban systems; urban systems, and industrial systems.

Apart from the application, typically the distribution system is radial in nature, including feeders and laterals. Some loads directly in MV level or in LV level are one- or two-phase loads. The majority of distribution circuits are three phase, although in some rural areas single-phase circuits may be used.

Generally, distribution networks are radial systems supplied from one step-down point. However, sometimes also closed-loop networks are used. Moreover, more and more frequently DG sources are connected to distribution networks. A similar effect is observed during a fault introducing motor loads. This is due to the

fact that motors behave as generators just after the fault inception. Similarly, if there are motor load taps along a radial distribution line it is equivalent to a line connected to multiple energy sources [327].

### ***2.5.2 Methods of Neutral Grounding***

The fault current during a fault depends on the fault-loop impedance and the equivalent supplying voltage. In the case of a phase-to-phase fault the fault loop has small impedance and the fault current reaches a relatively high level. The total fault-loop impedance is basically determined by the longitudinal parameters of the line sections covered by the fault.

Phase-to-ground fault characteristics significantly depend on the type of the network neutral grounding (grounding). System grounding, or the intentional connection of a phase or neutral conductor to ground, is used for the purpose of controlling the voltage to ground (earth), within predictable limits. It also provides for a flow of current that will allow detection of an unwanted connection between system conductors and ground (a phase-to-ground fault). The question of how the network neutral shall be grounded is determined by particular regulations. Local utility practice also influences the choice of the neutral-grounding arrangement on the MV circuits. The general purpose of grounding is to protect life and property in the event of faults and transient phenomena resulting from switching operations. Another reason for adequate grounding of the network is to allow high sensitivity of the relays operation. Fault detection and location invariably relies on the presence of a considerable amount of fault current and this is met in the solidly grounded networks or when the grounding impedance is small – as far as a fault between one or more phases and ground is considered.

Regarding the method of the neutral grounding, the MV networks can be divided into the following categories [96, 97, 265, 327]:

- directly or solidly grounded;
- network grounded through impedance; and
- isolated network.

Adequate method can be assured by grounding the star point delta/bye step-down transformer (Fig. 2.34a). In the case when the MV side of the transformer has delta connection, a separate grounding zigzag connected transformer is applied as a, generally, more efficient solution (Fig. 2.34b).

In the solidly grounded network the only impedance between the neutral and ground is that represented by the grounding transformer impedance, grounding conductor and the ground plate itself (Fig. 2.34). Solid neutral grounding is cheaper as it requires no extra equipment but can lead to high ground-fault currents that may cause damage and high step or touch voltages. On the other hand, this solution establishes a low-impedance path for ground-fault currents and hence satisfactory operation of relay protection.

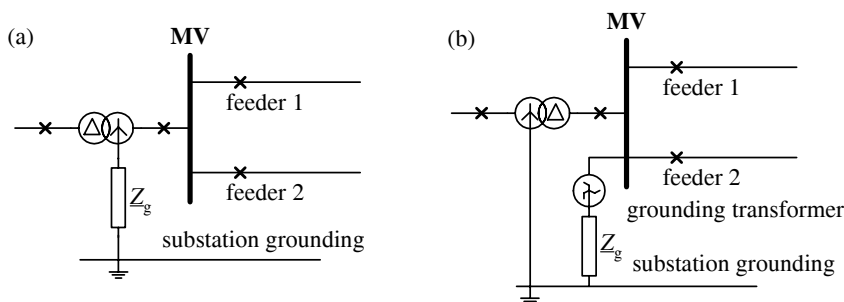


**Fig. 2.34** Methods of MV network grounding: (a) with delta-wye step-down grounding transformer; and (b) with grounding zigzag connected transformer;  $Z_g$  – grounding impedance

If the grounding impedance  $Z_g$  is intentionally selected for reducing a phase-to-ground fault, the grounding becomes non-effective (Fig. 2.35). For high grounding impedance the network capacitance plays a significant role.

There are two types of impedance grounding [96, 278]:

- grounding through resistor; and
- grounding through arc-suppressing coil (Petersen coil).

Resistance grounding is broadly dividing into two categories: high-resistance (when the fault current is limited to about 10 A) and low-resistance grounding (with fault current of some hundreds of amps). Generally, the high grounding resistance decreases the selectivity of the protective relays because the fault detection and the fault-place estimation are less accurate.

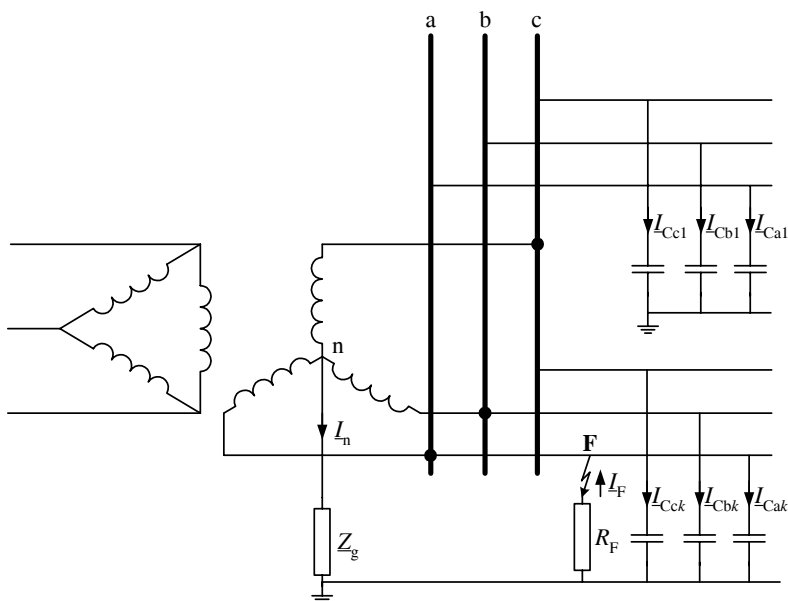


**Fig. 2.35** Equivalent scheme of network grounding through impedance

Grounding the neutral through the Petersen coil is used for reducing the capacitive current in isolated networks. The adequate inductance in the neutral is selected for compensation of the capacitive current during a phase-to-ground fault; thus this method is also known as the ground-fault compensation method. The equivalent scheme for this arrangement is shown in Fig. 2.36. The coil reactance is adjustable in relatively coarse steps, to allow for changes in network zero-sequence capacitance resulting from the switching out of lines. If the coil inductance exactly matches the system capacitance, the fault current has resistive character and may be insufficient for selective relay operation. Frequently, the grounding equipment is completed with a resistor ( $R_g$  in Fig. 2.36) that, with some delay, automatically paralleling the coil what permits fault current sufficient to correct relay operation.

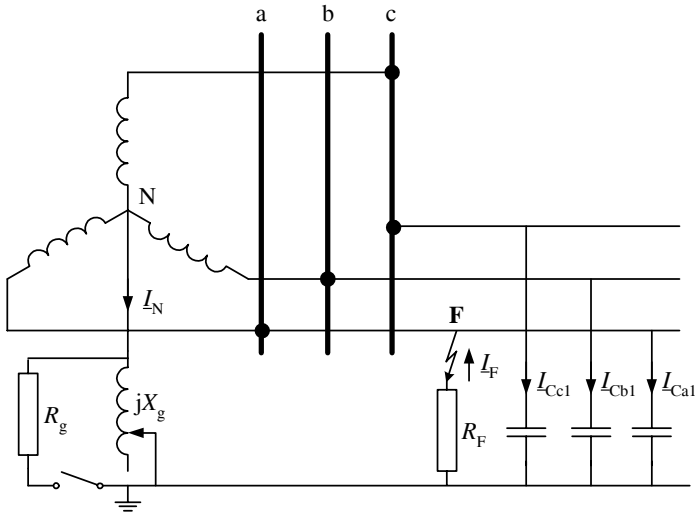


**Fig. 2.36** Equivalent scheme of the network grounding through a Petersen coil

An isolated network is one in which there is no intentional connection between the circuit and ground (Fig. 2.37). The currents during single phase-to-ground faults are low and depend mostly on the phase to ground capacitances of the lines.

The voltage between faulted equipment and ground is small, which improves safety. However, transient and power-frequency overvoltages can be higher than those obtained for other type of neutral grounding. Moreover, a one-phase grounding results in the full line-to-line voltage appearing on the other two sound phases. This situation can frequently cause failures in motors and transformers, due to insulation breakdown. There are known difficulties in detecting and locating the first line-to-ground fault: the overcurrent principle is not suitable here because the capacitive current in a sound line may be even greater than that measured at the faulted line [95, 97].

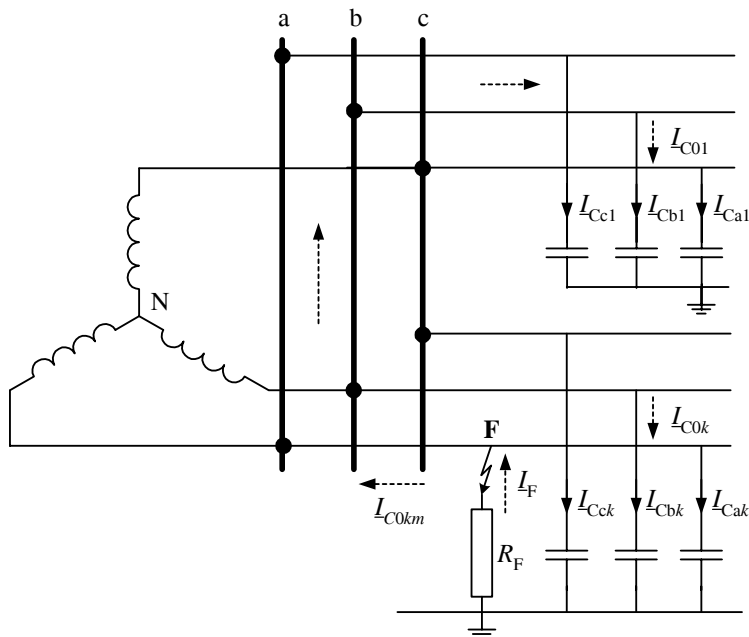


Fig. 2.37 Equivalent scheme of the isolated network; dotted lines show path for the fault current

### 2.5.3 Network Representation

Distribution networks are different from transmission and sub-transmission systems in the following characteristics:

- they operate at lower voltages than transmission lines;
- they are usually used radially;
- they usually have tapped loads along the line, not just at the terminals (where the measurements are available); and
- due to no line transposition and single-phase lateral and load, such networks usually should be considered as unbalanced networks.

Usually we consider a distribution system as a three-phase main line with lateral branches, some of which may be one- or two-phase circuits. Frequently, the system is wye connected with a ground at the supply transformer and often with multiple additional neutral grounds. The method of the neutral grounding has a considerable influence on the value and character of the phase-to-ground fault current. Practically, the impedance-based fault-location algorithms for phase-to-ground faults can be used only in effectively grounding network. On the other hand, the grounding method does not influence the accuracy for the other types of faults (as for example phase-to-phase).

The above-mentioned remarks are particularly important for cable networks. In branching points or laterals along the feeders, the cable sheaths are connected together and, generally, grounded through different resistances (Fig. 2.38a). Cable sheaths usually remain connected even if the respective sections are disconnected (Fig. 2.38b). This causes different equivalent schemes for positive/negative and zero-sequence of the network.

The circuit model described earlier did not include the effects of frequency dependence of the circuit parameters. Although this is unlikely to be a problem for the overhead line sections, it is possible that some cable configurations may exhibit a frequency dependence in the range 50–300 Hz, due to, for example, the non-linearity of steel armor.

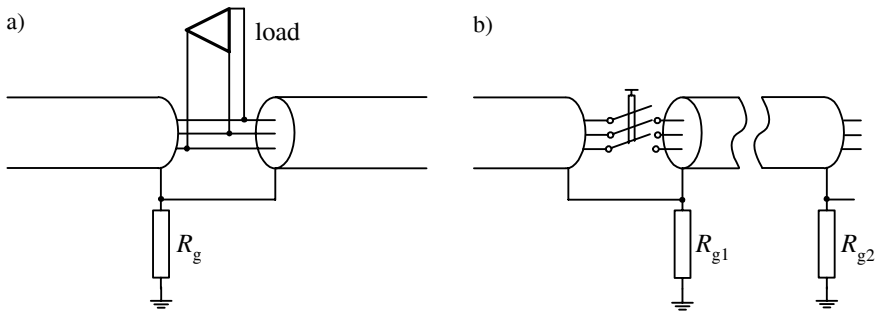


**Fig. 2.38** Cable-connection principle: (a) load connection; and (b) connection with switches

This could readily be incorporated into the circuit model using similar techniques adopted for time-domain solutions of frequency-dependent cable-parameter modeling [96, 97].

Fault Location on Power Networks

Saha, M.M.; Izykowski, J.J.; Rosolowski, E.

2010, X, 425 p., Hardcover

ISBN: 978-1-84882-885-8